Journal of Alloys and Compounds 735 (2018) 588–593

Contents lists available at ScienceDirect

Journal of Alloys and Compounds

journal homepage: http://www.elsevier.com/locate/jalcom

Review

High-quality strain-relaxed $Si_{0.72}Ge_{0.28}$ layers grown by MBE-UHV/CVD combined deposition chamber

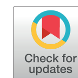

Dongfeng Qi [a, b, d, *, 1], Hanhui Liu [b, c, 1], Donglin Huang [a], Letian Wang [d], Songyan Chen [b, **], Costas P. Grigoropoulos [d]

[a] Laboratory of Infrared Materials and Devices, The Research Institute of Advanced Technologies, Ningbo University, Ningbo, Zhejiang, 315211, People's Republic of China
[b] Semiconductor Photonics Research Center, Department of Physics, Xiamen University, Xiamen, 361005, People's Republic of China
[c] Department of Materials Sciences and Engineering, University of California, Los Angeles, Los Angeles, CA 90095, USA
[d] Laser Thermal Lab., Department of Mechanical Engineering, University of California, Berkeley, Berkeley, CA 94720-1740, USA

ARTICLE INFO

Article history:
Received 27 June 2017
Received in revised form
23 October 2017
Accepted 7 November 2017

Keywords:
SiGe virtual alloys
UHV/CVD and MBE technology
2D materials

ABSTRACT

Surface smoothness and fully strain-relaxation $Si_{0.72}Ge_{0.28}$ virtual layer on Si(100) substrate with an inserted low temperature Ge flat layer is grown by combining molecular beam epitaxy system (MBE) and ultrahigh vacuum chemical vapor deposition system (UHV/CVD) in one vacuum chamber. The epitaxial SiGe layer with surface root-mean-square roughness of 1.22 nm and threading dislocation density of $1.5 \times 10^5 cm^{-2}$ is obtained. The influence of low temperature Ge interlayer on the high quality of SiGe epilayer is investigated. Both of the thermal stability and surface morphology of $Si_{0.72}Ge_{0.28}$ virtual layer are much better than that of SiGe layer grown by traditional UHV/CVD system.
© 2017 Elsevier B.V. All rights reserved.

Contents

1. Introduction 588
2. Experimental details 589
3. Results and discussion 589
4. Conclusions 592
Acknowledgments 593
References 593

1. Introduction

High-quality, tensile strained SiGe/Ge superlattice and Ge epitaxial layer have attracted a great deal of attention due to their band gap modification, high electron-hole mobility and promising device applications, which can be used as tensile strained Si/SiGe quantum well infrared photo detectors and strained-Ge metal-oxide-semiconductor field-effect transistor [1–3]. So many groups have focused on this promising area due to the high performance of these strained structures. However, how to achieve strained and single crystal SiGe and Ge layers are big problems for growing technology [4], firstly, it is very hard to grow single crystal SiGe/Si superlattice and strained Ge layer on Si substrate due to the large lattice mismatch between Si and Ge. Besides, the lattice of Si is smaller than that of SiGe and Ge, so it is hard to grow tensile strained SiGe/Si superlattice and SiGe layers directly on Si substrate.

Since the lattice constant of the Si_xGe_{1-x} alloy can be

* Corresponding author. Laboratory of Infrared Materials and Devices, The Research Institute of Advanced Technologies, Ningbo University, Ningbo, Zhejiang, 315211, People's Republic of China.
** Corresponding author.
E-mail addresses: qidongfeng@nbu.edu.cn (D. Qi), sychen@xmu.edu.cn (S. Chen).
[1] These authors contributed equally to this work.

https://doi.org/10.1016/j.jallcom.2017.11.105
0925-8388/© 2017 Elsevier B.V. All rights reserved.

continuously varied by changing the Ge content in the alloy, strain-relaxed and high Ge content Si_xGe_{1-x} virtual film on Si can be used as a virtual substrate. Since, the Si_xGe_{1-x} virtual substrate can provide significant band gap engineering freedom and offer a way of fabrication both compressive- and tensile-strained SiGe/Si superlattice for optoelectronic devices. In this case, the performance of the strained SiGe/Ge superlattice device depends strongly on the crystalline quality and surface morphology of the Si_xGe_{1-x} virtual substrate. Considerable efforts have been made to grow high-quality strain-relaxed Si_xGe_{1-x} virtual films on Si [5–10], such as compositionally forward- and reverse-graded buffer layer, low temperature (LT) interlayer, nano-scale patterned Si structures and ion implantation technology. Among these methods, the idea of the LT-Ge interlayer is widely adopted due to the simplification of growth condition.

The Ge interlayer, grown at low temperature, can be served as a low-energy center of defects. With the help of the defects, the strain in the SiGe layer can be fully relaxed at the interface of Si_xGe_{1-x} film and LT-Ge layer. In this case, low temperature technique is a promising method and widely utilized for molecular beam epitaxy (MBE) system. Thin, high quality and high-Ge content SiGe buffers are successfully fabricated by this technology. As these Si_xGe_{1-x} films are relatively thick, and the growth rates of MBE system is only about 0.1–0.5 A/s [11], it is very hard to grow thick Si_xGe_{1-x} layer, whereas rates of 5–10 nm/s are easily achievable by ultrahigh vacuum chemical vapor deposition (UHV/CVD), besides, it also has high throughput and in situ doping capabilities, so the growth rate is very high in CVD system. Though the growth rate is fast for this technology, the crystalline quality and the surface morphology are poor for both of Si_xGe_{1-x} and LT-Ge interlayer at low temperature by UHV/CVD system [12,13]. The method of combining MBE and UHV-CVD system for the growth of SiGe layers was reported before. Although these results have provided some impressive values, for instance, TDD of $3.4 \times 10^5 cm^{-2}$ with the RMS of 1.2 nm was found in $Si_{0.4}Ge_{0.6}$ layer by low temperature MBE technology [14], and $Si_{0.8}Ge_{0.2}$ with TDD of 6×10^4 cm^{-2} was achieved by RP-CVD [15,16], all of these references were mainly focus on surface morphologies and crystal quality of the SiGe films, and they did not give a systematic research of the effect of LT-Ge layer when the upper SiGe layer depositing.

In this paper, we combined MBE system and UHV/CVD in one chamber. Firstly we deposited the thin and flat LT-Ge interlayer on Si substrate (100) by the MBE technology, and then we combined advantages of UHV/CVD method and experimentally got surface smooth and relaxed $Si_{0.72}Ge_{0.28}$ layers on the LT-Ge interlayer. And their layers are uniform and indeed we have examined specimens from different points across the whole wafer.

2. Experimental details

In this system, there is a chamber ultra high vacuum chemical vapor deposition (UHVCVD). The chamber is equipped with eight-growth road gas source pipelines, and has two solid source beam source furnaces (MBE system). Besides, this system has advantages that the gas source and the solid state source can be alternately or mixed grown. Fig. 1 is a schematic representation of the growth system developed, installed and used in this work. The chamber is connected to pumping systems allowing a base pressure of 10^{-10} Torr. While system is under the UHVCVD mode, the working pressure range is between 10^{-2} and 10^{-6} Torr. Pure Si_2H_6 and GeH_4 are used as precursors being injected through mass flow/baratron flux/pressure controllers and decomposed at the substrate surface. The material of the hot-plate is Graphite, the mode is non-contract, and the plate can be heated from room-temperature to 1200 °C.The substrate temperature is measured by the thermocouple technology, and the accuracy of the heating temperature is 1 °C in this system. While system is under the MBE mode, a working pressure typically in the 10^{-7}–10^{-5} Torr range. Silicon and Germanium are generated from valved effusion cells which can be heated to 1200 °C. Silicon and Germanium beam deposit on the surface of substrate through the valve of cells. A reflection high-energy electron diffraction (RHEED) is used to monitor the growth processes.

The virtual substrate is epitaxially grown on a 4 inch n-type Si (100) wafer with resistivity of 0.1–1 Ω cm. Firstly, the wafer is cleaned by Radio Corporation of American (RCA) method and dried by N_2 before loading into the growth chamber. And then, the wafer is baked at 900 °C for 30 min to de-oxide. After that, low-temperature Ge (LT-Ge) is grown by using MBE mode. The purity of Ge beam source is 99.999%. The effusion cell can be heated to 1100 °C, and the working pressure range is between 10^{-7} and 10^{-5} Torr. Samples are divide into four groups, substrate temperature are room temperature, 150 °C, 180 °C, 200 °C respectively. Then, chamber is switched into UHVCVD system, and 50 nm and 250-nm-thick $Si_{0.72}Ge_{0.28}$ layers can be deposited on LT-Ge layer with the same flux ratio of Si_2H_6:GeH_4 = 3:5 at 400 and 500 °C, respectively. The higher temperature firstly may result in the Ge layer unstable, leading to the unsmooth surface of the upper SiGe layer. Secondly, the LT-Ge deposited by MBE method is not only has the flat surface morphology, but also contains many point defects on the surface. As a result, the threading dislocations can be captured by surface point defects of LT-Ge, leading to the dislocation pinning at the interface. For the LT-SiGe layer, there are also some point defects can be formed, which can also capture the threading dislocations, in this condition, lower TDD SiGe layer can be formed by this method. The surface morphology is analyzed by atomic force microscopy (AFM) using Seiku Instruments SPI4000/SPA-400 system operating in tapping mode. The Ge content in SiGe film and the degree of strain relaxation are evaluated by high-resolution X-ray diffraction (HRXRD) and Raman scattering spectrum. Symmetric (004) and asymmetric (224) Omega–2theta measurements are performed at room temperature in the Bede, D1 system, by using a Cu Kα1 (λ = 0.15406 nm) radiation. Raman scattering measurements are carried out at room temperature using the backscattering geometry with 532 nm Ar^+ line as the excitation source. The vertical distribution of Si and Ge in the samples is tested using Auger electron spectrum (AES). The depth profile of threading dislocation density is measured by counting pits formed from selectively chemical etching and the detail distribution of these threading dislocations are captured by Transmission electron microscope (TEM).

3. Results and discussion

To study the effect of LT-Ge interlayer, a reflection high-energy electron diffraction (RHEED) images are recorded in real-time to monitor the LT-Ge and SiGe surface. In the white block scheme of Fig. 1 are AFM images and corresponding RHEED of LT-Ge layer. After the deposition of Ge layer at room temperature (Fig. 2(a)), there is no pattern shown in the RHEED, which means only amorphous Ge can be formed in this condition. Besides, island structures appear on the surface, and the LT-Ge islands act as the strain-accommodating layer where strain energy stemming from the lattice mismatch between Si and Ge is relieved via formation of systematic misfit dislocations. With the increasing of deposition temperature, the RHEED patterns exhibit a weak 2 × 1 streaks (Fig. 2(b)), and finally a well-developed longitudinal 2 × 1 streaks are rebuilt (Fig. 2(c)), This pattern is related to the two-dimensional (2D) growth of the Ge layer [17], and the root-mean-square (RMS) is 0.61 nm, which means the growth mode switches from three-

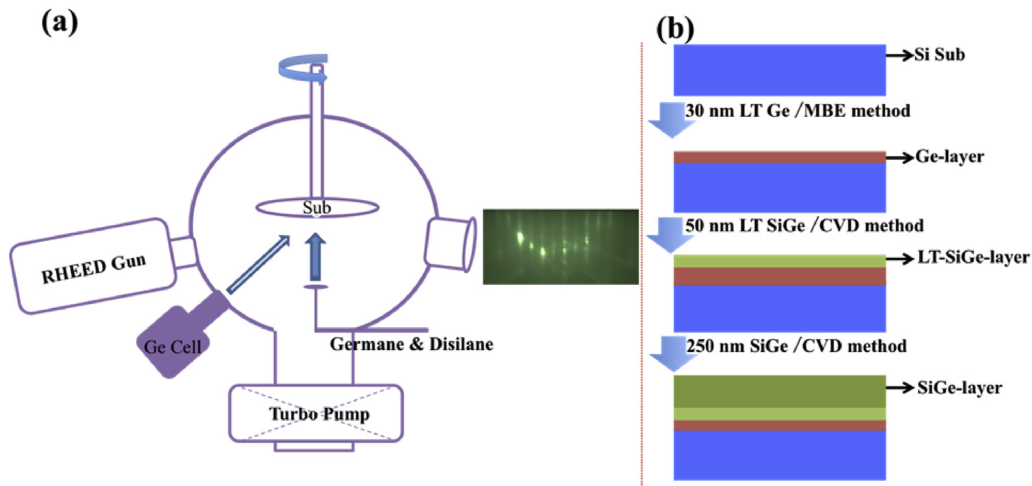

Fig. 1. (a) Schematic diagram of the MBE&UHV/CVD system; (b) Schematic diagram of the cross section of the $Si_{0.72}Ge_{0.28}$ virtual substrates by MBE&UHV/CVD system.

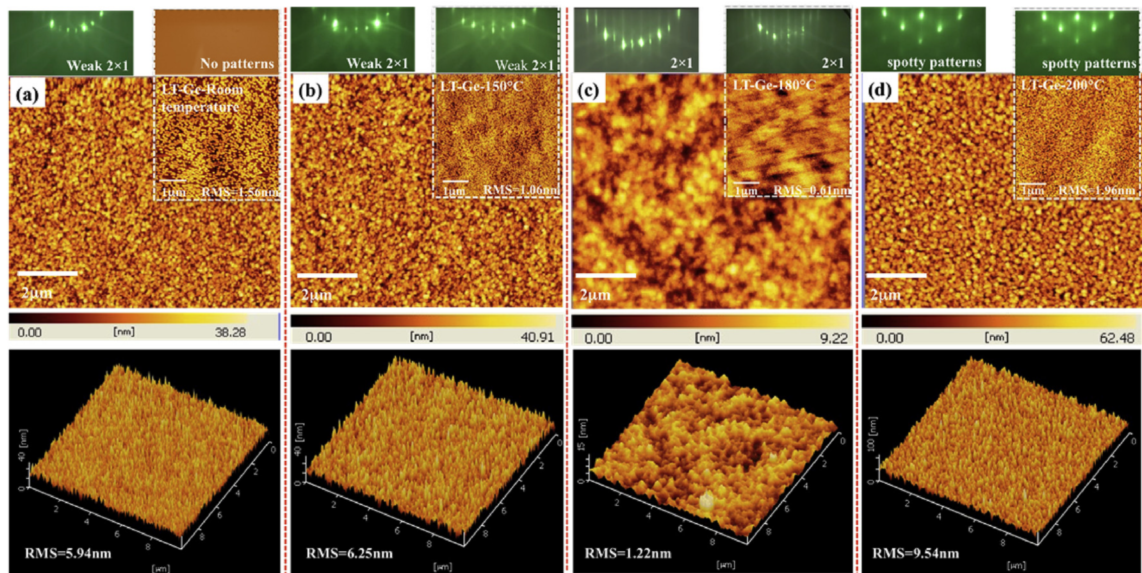

Fig. 2. The RHEED patterns and AFM images of the SiGe layers with LT Ge layers at different epitaxy temperatures; the white block diagrams are RHEED patterns and AFM images of the corresponding LT Ge layers; the upper SiGe layer growth condition: a 50 nm low-temperature $Si0_{0.72}Ge_{0.28}$ layer was deposited at 450 °C, and then a 200-nm-thick $Si0_{0.72}Ge_{0.28}$ top layer was grown at 500 °C. (a–d) are AFM images and corresponding RHEED patterns of SiGe layer under different LT-Ge growth condition.

dimensional (3D) to 2D mode [18]. If the deposition temperature is above 200 °C, 3D island structures will appear on the surface again, as shown in Fig. 2(d), and RHEED pattern showed spots appearing along 1 × 1 streaks. Generally, film growth is governed by a series of events in a deposit process: adsorption or capture of the impinging molecules, surface diffusion and association of the molecules leading to nucleation and growth. When the temperature of the substrate is not enough for the sufficient surface diffusion, as the situation of Fig. 2(a–b), the molecules will turn to aggregate result in some isolate islands. On the other hand, with the increase of temperature of the substrate, the adsorption rate of the impinging molecules increases, and if the adsorption rate is too high to match the diffusion rate, as a result, the surface will come into rough, as shown in Fig. 2(d).

When switching to UHV/CVD part, pure Si_2H_6 and GeH_4 are used as precursors and can be decomposed on the LT-Ge interlayer, and the growth rate is about 2.7 nm/s. Firstly, 50-nm thick low temperature $Si_{0.72}Ge_{0.28}$ layer is deposited at 450 °C. This LT-SiGe layer is used to prevent the interfusion between the LT-Ge and the upper SiGe layer, and reduce forming threading dislocations. Then, 250 nm thick $Si_{0.72}Ge_{0.28}$ top layer is grown at 500 °C. The surface morphology of the SiGe layers with LT Ge layers at different epitaxy temperatures are shown in Fig. 2. After investigating the AFM images and RHEED, it reveals that the surface morphology of the underneath layer plays a key role for the quality of the upper SiGe layer. Compared with the other samples, The RMS of sample with LT-Ge temperature deposited at 180 °C is only 1.22 nm, and a well-developed longitudinal 2 × 1 streaks also appears.

Fig. 3(b) shows symmetric (004) and asymmetric (224) rocking curves of SiGe layer with LT Ge layers deposited at 180 °C. The rocking curves reveal three significant peaks attributed to the Si substrate, SiGe layers and LT-Ge layer, and the line shape of the broad peak is quite symmetric, implying that the sample is superior in the crystalline quality [13–16]. Analysis shows that Ge

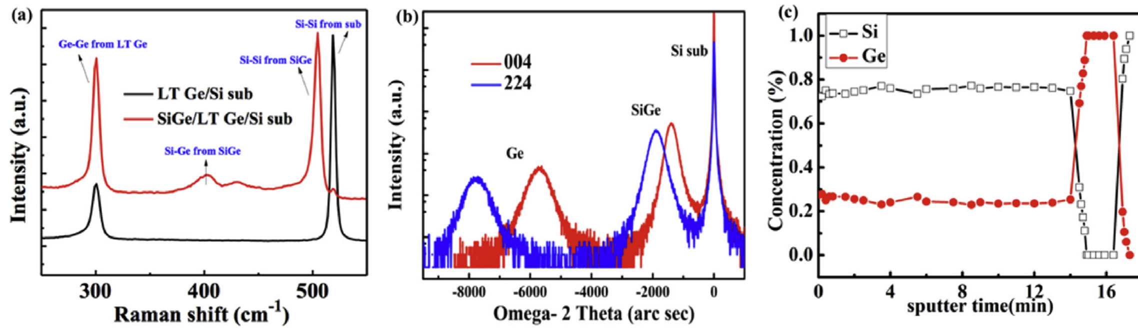

Fig. 3. The composition analysis of the SiGe virtual substrate with LT Ge layer deposited at 180 °C; (a) The Raman spectra of the SiGe layer; (b) HRXRD rocking curves of the SiGe film; (c) The Auger electron spectroscopy (AES) of the SiGe layer.

composition is 0.28 and the degree of strain relaxation is 95% for the SiGe layer, 97% for the low temperature Ge layer, which is much similar with that of Raman spectra (The Ge content and degree of strain relaxation in SiGe layer is 0.29 and 93%, and strain relaxation of LT-Ge is 98%, respectively), as shown in Fig. 3(a). The longitudinal distribution of the elements in SiGe virtual substrate can be investigated from Auger electron spectroscopy (AES), as shown in Fig. 3(c), The interface between LT Ge interlayer and SiGe layer is sharp, proving that the inter-diffusion between the LT Ge and SiGe epitaxial layer is inconspicuous, and the uniform distribution of Ge in the SiGe layer shows the average component of Ge is about 0.3, which is consistent with the Raman and XRD results. With the analyzing of Raman, XRD and AES results, we find that the SiGe virtual substrate deposited by the MBE-UHV/CVD system have the sharp interface and the uniform distribution of the element.

For the SiGe virtual substrate, the threading dislocation density (TDD) is the essential measure on the material quality. To make sure the exact information on the SiGe virtual substrate, the top SiGe layer are removed by chemical etching ($HF:K_2Cr_2O_7:H_2O_2 = 6\ ml:4g:180\ ml$) through controlling etching time, the etching speed was about 44 nm/min. Each dislocation density is average values by counting etch pits in 3–5 pictures across the surface and only one typical picture is displayed. Fig. 4(a) shows typical optical image of SiGe surface on LT-Ge after Secco etching, and the threading dislocation density near the SiGe surface is only $1.5 \times 10^5 cm^{-2}$. When the etching depth equal to 44 nm, the TDD is about $5.6 \times 10^5\ cm^{-2}$. With the increase of etching depth, the density of TDD also increases. The TDD is about $1.2 \times 10^7\ cm^{-2}$ when the etching depth equals to 200 nm. Compare with the result of transmission electron microscope (TEM), as shown insert image of Fig. 4(a), it reveals that most of the threading dislocations are located around the interface of LT Ge and SiGe layer (200–250 nm). Besides, We repeated our experiment and measurements several times and the RMS and the TDD of the virtual sub did not changed much, as shown in Fig. 5. From above discussions, we know that the LT-Ge deposited by MBE method not only has the flat surface morphology, but also contains many point defects on the surface. As a result, the threading dislocations can be captured by surface point defects of LT-Ge, leading to the dislocation pinning at the interface. In this condition, lower TDD SiGe layer can be formed by this method.

We also deposite the SiGe layer with the same system using only UHV/CVD for comparison. For the SiGe virtual substrate, we optimize the growth condition, and characteristics of SiGe virtual substrate show that Ge composition is 0.31, the degree of strain relaxation is 143% for the SiGe layer, 112% for the low temperature

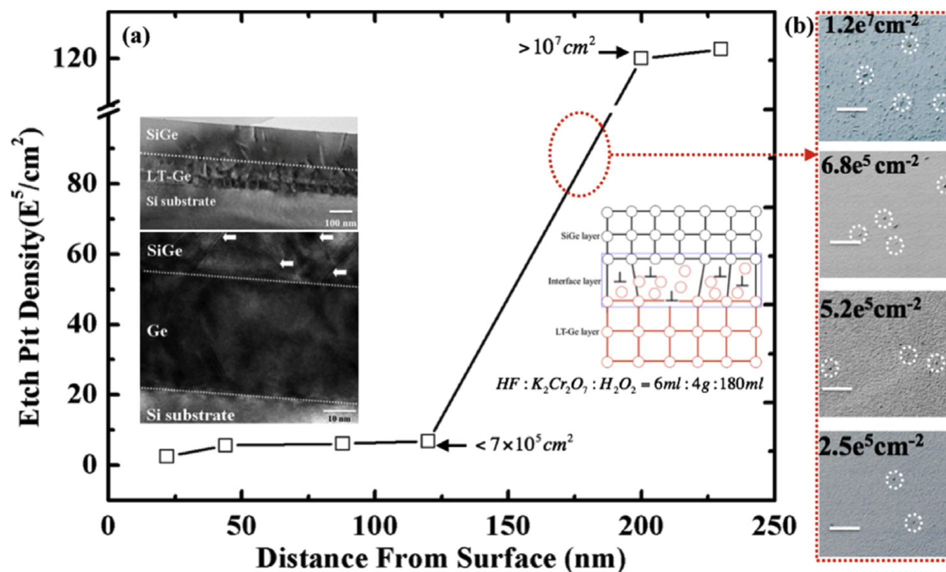

Fig. 4. Depth profile of TDD in SiGe/Ge epilayer on Si substrate, the insert images are schematic image of SiGe/Ge interface, a high-resolution TEM image around the Ge/SiGe interface and a wide-area TEM image of the SiGe virtual layer, and white arrows in TEM images are threading and misfit dislocations; (b) Optical images of SiGe layer etched at various depths to reveal etch pit density.

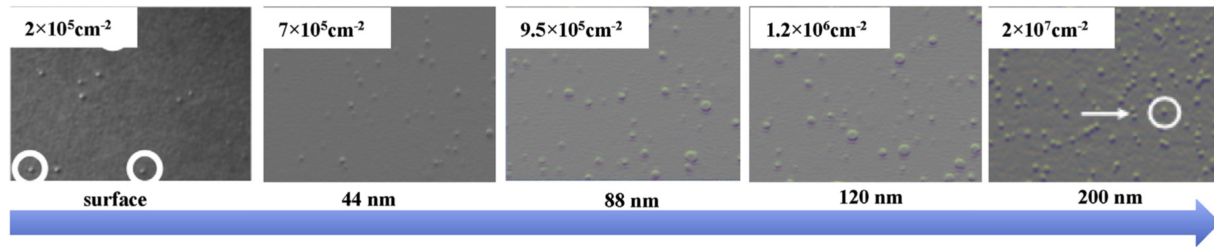

Fig. 5. Depth profile of TDD in SiGe/Ge epilayer on Si substrate, and the optical images of SiGe layer etched at various depths to reveal etch pit density. The growth condition is the same as that of the condition reported in the manuscript.

Ge layer and the RMS is about 1.87 nm, and all of these parameters are much larger than that of ours results, as shown in Fig. 6. To further study the stability of the SiGe films at higher temperatures, thermal annealing is conducted at different temperature for 30 min in N_2 ambient, which is shown in Fig. 6. The RMS of the SiGe virtual substrate which grown by the MBE&UHV/CVD does not change much as annealing temperature increasing. Oppositely, the surface morphology of the SiGe layer grown by UHV/CVD system changes much as the annealing temperature increasing. There are two main reasons result in this phenomenon. Firstly, The residual strain in the layer can be released after annealing, and this processing can lead to the increasing of the threading dislocations, which causes the change of the surface morphology. The as-grown sample (MBE&UHV/CVD) is nearly full relaxation, and there are not so many threading dislocations produce after annealing, so the surface is still smooth after annealing [19–22]. Secondly, the interface of the LT-Ge and SiGe layer is another key role for the surface morphology. From TEM we know that the interface is very clean, which can reduce the inter-mixing of the LT-Ge and SiGe layer when annealing.

4. Conclusions

The hybrid epitaxy method with the MBE and UHV/CVD is introduced to the epitaxy of SiGe virtual substrates with a thin Ge interlayer. Firstly, the LT Ge layer deposited by MBE provides the flat

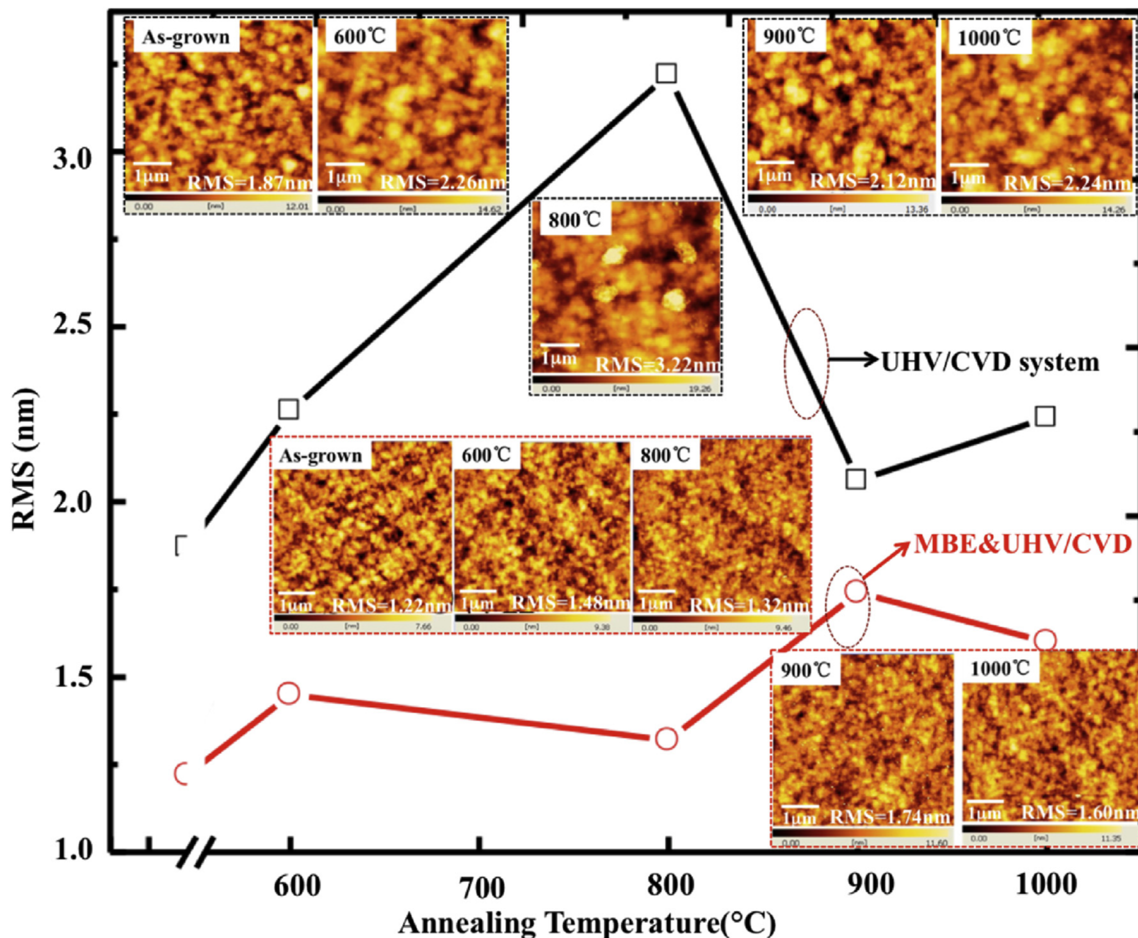

Fig. 6. The table shows the RMS, TDD and strain relaxation comparison of SiGe virtual layers grown by UHV/CVD and MBE&UHV/CVD system. The bottom image shows the RMS comparison and the corresponding AFM images showing the surface morphology of SiGe virtual layers after annealed at different temperature; those samples are annealed at different temperatures for 0.5 h.

base for the epitaxy of the SiGe layer. Point defects in the interface can capture the dislocations and reduce the propagation of threading dislocations. Secondly, the high temperature of the SiGe layer deposited by UHV/CVD not only increases the epitaxy speed but also promotes the SiGe layer lattice relaxation, leading to a fully relaxed and high thermal stability SiGe virtual substrate. The investigation provides us a new method to grow the multilayer materials.

Acknowledgments

This work was supported by the Natural Science Foundation of China under Grant number 61705117 and 61534005, and sponsored by K. C. Wong Magna Fund in Ningbo University.

References

[1] L.L. Minjoo, E.A. Fitzgerald, M.T. Bulsara, M.T. Currie, A. Lochtefeld, J. Appl. Phys. 97 (2005) 011101.
[2] K. Kato, N. Taoka, M. Sakashita, O. Nakatsuka, S. Zaima, Appl. Phys. Lett. 107 (2015) 102102.
[3] G.L. Luo, Y.C. Hsieh, E.Y. Chang, M.H. Pilkuhn, C.H. Chien, T.H. Yang, C.C. Cheng, C.Y. Chang, J. Appl. Phys. 101 (2007) 084501.
[4] M.T. Currie, S.B. Samavedam, T.A. Langdo, C.W. Leitz, E.A. Fitzgerald, Appl. Phys. Lett. 72 (1998) 1718.
[5] E.A. Fitzgerald, Y.-H. Xie, M.L. Green, D. Brasen, A.R. Kortan, J. Michel, Y.-J. Mii, B.E. Weir, Appl. Phys. Lett. 59 (1991) 811.
[6] J.P. Liu, L.H. Wong, D.K. Sohn, L.C. Hsia, L. Chan, C.C. Wong, H.J. Ostenc, Electrochem. Solid-State Lett. 8 (2005) G60.
[7] L.H. Wong, J.P. Liu, C. Ferraris, Appl. Phys. Lett. 88 (2006) 041915.
[8] J.H. Li, C.S. Peng, Y. Wu, D.Y. Dai, J.M. Zhou, Z.H. Mai, Appl. Phys. Lett. 71 (1997) 3132.
[9] M. Bauer, K. Lyutovich, M. Oehme, E. Kasper, H.-J. Herzog, F. Ernst, Thin Solid Films
369 (2000) 152.
[10] K. Sawano, S. Koh, Y. Shiraki, Y. Ozawa, T. Hattori, J. Yamanaka, K. Suzuki, K. Arimoto, K. Nakagawa, N. Usami, Appl. Phys. Lett. 85 (2004) 2514.
[11] D.V. Yurasov, M.N. Drozdov, N.D. Zakharov, A.V. Novikov, J. Cryst. Growth 396 (2014) 66–70.
[12] D.H. Choi, Y.S. Ge, James S. Harris, J. Cagnon, S. Stemmer, J. Cryst. Growth 310 (2008) 4273–4279.
[13] Z. Zhou, Z. Cai, C. Li, H. Lai, S. Chen, J. Yu, Appl. Surf. Sci. 255 (2008) 2660–2664.
[14] M. Myronov, et al., Appl. Phys. Lett. 94 (2009) 092108.
[15] Bogumilowicz, et al., J. Cryst. Growth 283 (2005) 346–355.
[16] Dobbie, et al., Semicond. Sci. Technol. 25 (2010) 085007.
[17] S. Kidowaki, T. Asano, Y. Shimura, M. Kurosawa, N. Taoka, O. Nakatsuka, S. Zaima, Thin Solid Films 598 (2016) 72–81.
[18] S. Das, Krista R. Khiangte, Rajveer S. Fandan, Jaswant S. Rathore, Ravindra S. Pokharia, S. Mahapatra, Apurba Laha, Curr. Appl. Phys. 17 (2017) 327–332.
[19] N. Sugii, J. Appl. Phys. 89 (2001) 6459.
[20] R. Kube, H. Bracht, J.L. Hansen, A.N. Larsen, E.E. Haller, S. Paul, W. Lerch, J. Appl. Phys. 107 (2010) 073520.
[21] P. Zaumseil, et al., J. Appl. Phys. 76 (4) (1994) 2191.
[22] N.E.B. Cowern, et al., Phys. Rev. Lett. 72 (16) (1994) 2585.